energies

MDPI

Article

Thermal Performance Investigation of Slotted Fin Minichannel Heat Sink for Microprocessor Cooling

Taha Baig [1,2], Zabdur Rehman [3,*], Hussain Ahmed Tariq [4], Shehryar Manzoor [2], Majid Ali [1], Abdul Wadood [5], Krzysztof Rajski [6] and Herie Park [7,*]

1 Department of Mechanical Engineering, Wah Engineering College, University of Wah, Wah Cantt 47040, Pakistan; taha.baig@wecuw.edu.pk (T.B.); majidmaju995@gmail.com (M.A.)
2 Department of Mechanical Engineering, University of Engineering and Technology Taxila, Taxila 47080, Pakistan; m.shehryar@uettaxila.edu.pk
3 Department of Mechanical Engineering, Air University Islamabad, Aerospace and Aviation Campus, Kamra 43570, Pakistan
4 Department of Mechanical Engineering, Institute of Space Technology, Islamabad 44000, Pakistan; ahmedtariq90@gmail.com
5 Department of Electrical Engineering, Air University Islamabad, Aerospace and Aviation Campus, Kamra 43570, Pakistan; wadood@au.edu.pk
6 Faculty of Environmental Engineering, Wroclaw University of Science and Technology, 50-370 Wrocław, Poland; krzysztof.rajski@pwr.edu.pl
7 Department of Electrical Engineering, Dong-A University, Busan 49315, Korea
* Correspondence: zabd@aack.au.edu.pk (Z.R.); park.herie@gmail.com (H.P.)

Abstract: Due to high heat flux generation inside microprocessors, water-cooled heat sinks have gained special attention. For the durability of the microprocessor, this generated flux should be effectively removed. The effective thermal management of high-processing devices is now becoming popular due to high heat flux generation. Heat removal plays a significant role in the longer operation and better performance of heat sinks. In this work, to tackle the heat generation issues, a slotted fin minichannel heat sink (SFMCHS) was investigated by modifying a conventional straight integral fin minichannel heat sink (SIFMCHS). SFMCHSs with fin spacings of 0.5 mm, 1 mm, and 1.5 mm were numerically studied. The numerical results were then compared with SIFMCHSs present in the literature. The base temperatures recorded for two slots per fin minichannel heat sink (SPFMCHS), with 0.5 mm, 1 mm, and 1.5 mm fin spacings, were 42.81 °C, 46.36 °C, and 48.86 °C, respectively, at 1 LPM. The reductions in base temperature achieved with two SPFMCHSs were 9.20%, 8.74%, and 7.39% for 0.5 mm, 1 mm, and 1.5 mm fin spacings, respectively, as compared to SIFMCHSs reported in the literature. The reductions in base temperature noted for three SPFMCHSs were 8.53%, 9.05%, and 5.95% for 0.5 mm, 1 mm, and 1.5 mm fin spacings, respectively, at 1 LPM, as compared to SIFMCHSs reported in the literature. In terms of heat transfer performance, the base temperature and thermal resistance of the 0.5 mm-spaced SPFMCHS is better compared to 1 mm and 1.5 mm fin spacings. The uniform temperature distribution at the base of the heat sink was observed in all cases solved in current work.

Keywords: slotted fin minichannel heat sink; base temperature; thermal management; numerical simulation

Citation: Baig, T.; Rehman, Z.; Tariq, H.A.; Manzoor, S.; Ali, M.; Wadood, A.; Rajski, K.; Park, H. Thermal Performance Investigation of Slotted Fin Minichannel Heat Sink for Microprocessor Cooling. *Energies* **2021**, *14*, 6347. https://doi.org/10.3390/en14196347

Academic Editor: Marco Marengo

Received: 24 August 2021
Accepted: 29 September 2021
Published: 4 October 2021

1. Introduction

With the rapid development in the information technology sector, the thermal management of electronic devices is becoming essential due to the high generation of heat flux. The world is advancing rapidly towards compact devices; however, this presents the challenging task of the effective and timely removal of unwanted heat. Therefore, this problem has attracted many researchers to create efficient cooling techniques while avoiding any losses in functioning of the devices. The heat transfer can be increased either by enhancing the thermal physical properties of ordinary fluid or by optimizing the heat

sink surface to volume ratio. Previously, air was used for the removal of heat from the electronic devices, but it is now unable to remove high heat fluxes. Therefore, attention is now being focused upon liquid cooling techniques, due to their higher efficiency when compared to air.

Saeed and Kim [1] numerically investigated the thermal performance of a water-cooled straight fin minichannel heat sink with varying fin spacings, fin thicknesses, and fin heights. In 1981, Tuckerman and Pease [2], for the first time, circulated water directly through a microchannel. Huang et al. [3] numerically investigated the thermal performance of parallel, staggered, and trapezoidal stagger slotted microchannel heat sinks. Knight et al. [4] proposed a scheme to optimize the geometry of microchannels in both turbulent and laminar regions. Gawali et al. [5] used a straight microchannel heat sink to absorb a large quantity of heat. Wang et al. [6] suggested a numerical model to examine the thermal performance of a microchannel heat sink. They optimized the channel number, channel aspect ratio under a fixed pressure drop, volume flow rate, and pumping power. Hung et al. [7] investigated the thermal performance of a porous microchannel heat sink with rectangular, block, trapezoidal, thin rectangular, and sandwich distributions. Gunnasegaran et al. [8] studied the different geometrical effect on microchannel heat sinks. They found a high heat transfer coefficient using a rectangular shape followed by a trapezoidal and a triangular shape. Qu et al. [9] performed an experimental study on heat transfer enhancement in a trapezoidal silicon microchannel. Kumar and Singh [10] investigated pressure drop and heat transfer in a microchannel heat sink with a trapezoidal shape.

Minichannel heat sinks are popular due to lower pressure drops in comparison to microchannel heat sinks. Xie et al. [11] performed a numerical study for heat sinks with normal, mini, and microchannels with bottom dimensions of 20 mm $\times$ 20 mm, by using water as a coolant. Dixit and Gosh [12] performed an experimental study on minichannel heat sinks to investigate the thermal performance of diamond, offset, and straight heat sinks. They observed that the pressure drop for an offset minichannel is lower than in a diamond minichannel. Saini and Webb [13] found that an impinging flow can dissipate 94.4 W as compared to duct flow, which can dissipate 84 W. Naphon and Wiriyasart [14] studied the liquid cooling of a minichannel rectangular heat sink with and without a thermoelectric effect. They found that thermoelectric material has a great impact on CPU temperature, as well as on energy consumption. Saeed and Kim [15] performed both numerical and experimental studies on minichannel heat sinks with fin spacings of 0.5 mm, 1 mm, and 1.5 mm using Al_2O_3-H_2O nanofluids. Al-Taey et al. [16] investigated whether the CPU temperature has a direct relationship with the cooling fluid (water). They also noticed a direct relation of mass flow rate with heat transfer rate and Nusselt number but an inverse relation with thermal resistance. Yu et al. [17] performed both numerical and experimental studies to compare a plate fin heat sink with a plate-pin fin heat sink using air as a cooling fluid. Tariq et al. performed experimental and numerical studies to investigate the thermal performance of cellular structures using air [18], water [19], and nanofluids [20]. Valueva and Purdin [21] numerically investigated the effect of aspect ratio of a rectangular channel on pulsating flow dynamics. Valueva and Purdin [22] developed a numerical model for the heat exchange between stationary and pulsating laminar flow inside a rectangular channel.

Many interrupted fin geometries have reported achieving high heat transfer as compared to integral fin geometries. Khoshvaght-Aliabadi et al. [23] calculated the hydrothermal performance of plate and plate-pins in triangular, trapezoidal, and sinusoidal configuration in a minichannel. Rezaee et al. [24], in their numerical and experimental studies, evaluated the effects of variable pin length and longitudinal pitch in a pin-fin heat sink. Khoshvaght-Aliabadi et al. [25] found that the hydrothermal performance of an interrupted fin is higher as compared to integral fin geometry. Ali et al. [26], in their experimental and numerical studies, investigated the thermal performance of integral-fin and pin-fin heat sinks.

Many studies addressing the thermal performance of minichannel heat sinks can be found in the literature. However, work on minichannel slotted fin heat sinks using a numerical study is rare. In this study, the thermal performance of heat sinks with varying fin spacings of 0.5 mm, 1 mm, and 1.5 mm was numerically investigated. These fin spacings were selected from the literature, and these geometries were optimized by creating slots inside the heat sinks. These were named slotted per fin minichannel heat sink SPFMCHSs. These selected SPFMCHSs were then compared to the straight integral fin minichannel heat sink (SIFMCHS) present in the literature [1] using the same heating power of 325 W. In this study, the conventional SIFMCHS was replaced by a novel SPFMCHS, which had varying fin spacings. To the best of the authors' knowledge, none of the previously mentioned studies have reported the effect of slots and slot thickness in a minichannel heat sink with integral fin spacings of 0.5 mm, 1 mm, and 1.5 mm. Numerical simulations were performed using ANSYS Fluent as a solver. The Reynolds number range for this study was 1900, 2900, and 3800, respectively. Uniform temperature distribution was observed at the base of the heat sink. The selection of both the slot thickness and the number of slots was also discussed in detail.

2. Numerical Model

The problem of the conjugate heat transfer was solved numerically using ANSYS Fluent. Assumptions made in this study were as follows: incompressible flow, turbulent model (k-epsilon), no viscous heating, no inside heat generation, and the same thermal properties during the flow. Absolute velocity formulation was used, along with a pressure-based solver. For this study, transport equation K-ε, with realizable and standard wall functions, was used. Velocity and pressure coupling was controlled by a Semi-Implicit Method for Pressure-Linked Equations (SIMPLE). For pressure, a second-order spatial discretization scheme was used, while for the turbulent dissipation rate, turbulent kinetic energy, and discretization of momentum, a second order upwind scheme was used. The outlet was at zero gauge pressure. For the conjugate problem inside the solid region, velocities were zero everywhere [11,27]. The selected base temperature was 46.424 °C, and the inlet temperature was 27 °C. The following governing equations were used for the conservation of energy, mass, and momentum [28]. For validation, conventional SIFMCHSs with 1 mm spacing were solved numerically by applying the same methodology, and the results were then compared with the literature [1], as shown in Figure 1.

$$\frac{\partial}{\partial x_i}(\varrho u_i) = 0 \tag{1}$$

$$\frac{\partial}{\partial x_i}(\varrho u_i u_j) = -\frac{\partial \varrho}{\partial x_j} + \frac{\partial}{\partial x_i}\left[(\mu + \mu_t)\frac{\partial u_j}{\partial x_i}\right] + \frac{\partial}{\partial x_i}\left[(\mu + \mu_t)\frac{\partial u_i}{\partial x_j}\right], j = 1,\ 2,\ 3 \tag{2}$$

$$\frac{\partial}{\partial x_i}(\varrho u_i T) = \frac{\partial}{\partial x_i}\left[\left(\frac{\lambda}{c_p} + \frac{\mu_t}{\sigma_t}\right)\frac{\partial T}{\partial x_i}\right] \tag{3}$$

$$\frac{\partial}{\partial x_i}(\varrho k u_i) = \frac{\partial}{\partial x_i}\left[\left(\mu + \frac{\mu_t}{\sigma_k}\right)\frac{\partial k}{\partial x_i}\right] + G_k - \rho\epsilon \tag{4}$$

$$\frac{\partial}{\partial x_i}(\varrho \epsilon u_i) = \frac{\partial}{\partial x_i}\left[\left(\mu + \frac{\mu_t}{\sigma_\epsilon}\right)\frac{\partial \epsilon}{\partial x_i}\right] + \frac{\epsilon}{k}(c_1 G_k - c_2 \rho\epsilon) \tag{5}$$

where "k" is kinetic turbulence energy, "$\in$" is turbulence rate of dissipation and "G_k" is the generation of kinetic turbulence energy.

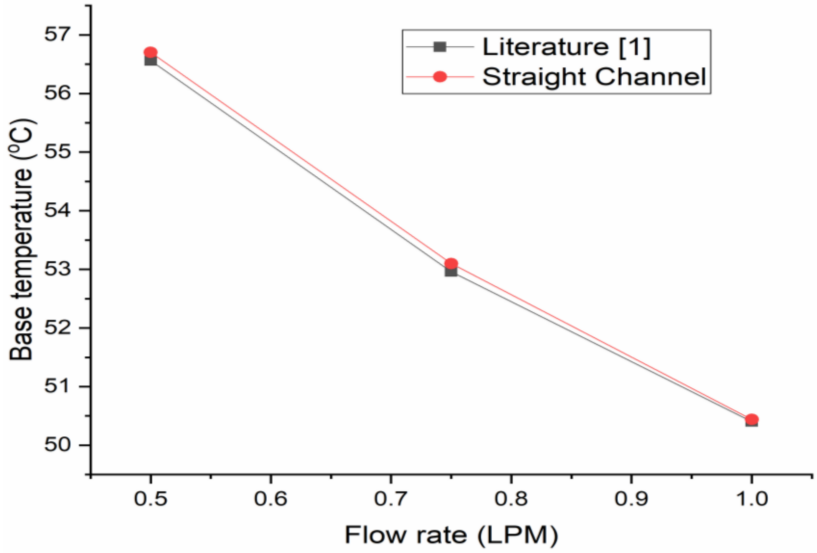

Figure 1. Validation of numerical model.

2.1. Boundary Condition

The following boundary conditions were used to solve the conjugate heat transfer problem:
No-slip conditions at the wall.
Uniform velocity was considered as the inlet of the heat sink

$$\text{At y} = \text{h},\ \text{u} = 0,\ \text{v} = -U_{in},\ \text{w} = 0 \tag{6}$$

Heat flux was provided at the bottom of the heat sink

$$\text{At y} = 0, -\lambda \frac{\partial T}{\partial y} = q \tag{7}$$

The right and left surface walls were considered as adiabatic.

$$\begin{array}{c} \text{At x} = 0,\ \frac{\partial t}{\partial x} = 0 \\ \text{At x} = \text{w}_\text{s},\ \frac{\partial t}{\partial x} = 0 \end{array} \tag{8}$$

The fluid inlet temperature was considered as constant

$$\text{At y} = \text{h}, \quad T = T_i \tag{9}$$

2.2. Data Reduction

The following procedure was adopted for data evaluation. The removal of heat from the heat sink was calculated using Equation (6).

$$\dot{Q} = \dot{m}\text{C}_\text{p}(T_o - T_i) \tag{10}$$

The log of mean temperature difference can be calculated from Equation (7).

$$\text{LMTD} = \frac{(T_b - T_i) - (T_b - T_o)}{\ln\left(\frac{(T_b - T_i)}{(T_b - T_o)}\right)} \tag{11}$$

Thermal resistance of the heat sink was calculated using Equation (8).

$$R_{th} = \frac{\text{LMTD}}{\dot{Q}} \tag{12}$$

2.3. Independent Mesh Study

An intensive study was carried out to ensure that the solution is independent of the mesh. The mesh is considered independent when the temperature difference (between the maximum base temperature and the inlet temperature) shows less than 1% deviation as shown in Figure 2. Six cases with a different number of elements were examined, the number of elements being 2138709, 2358425, 2525411, 2700599, 2912432, and 3102635. The results obtained for case 5 and case 6 were very close to each other, showing a deviation of 0.3% in temperature difference. The number of elements for case 5 was used for the entire study to save computation time and memory.

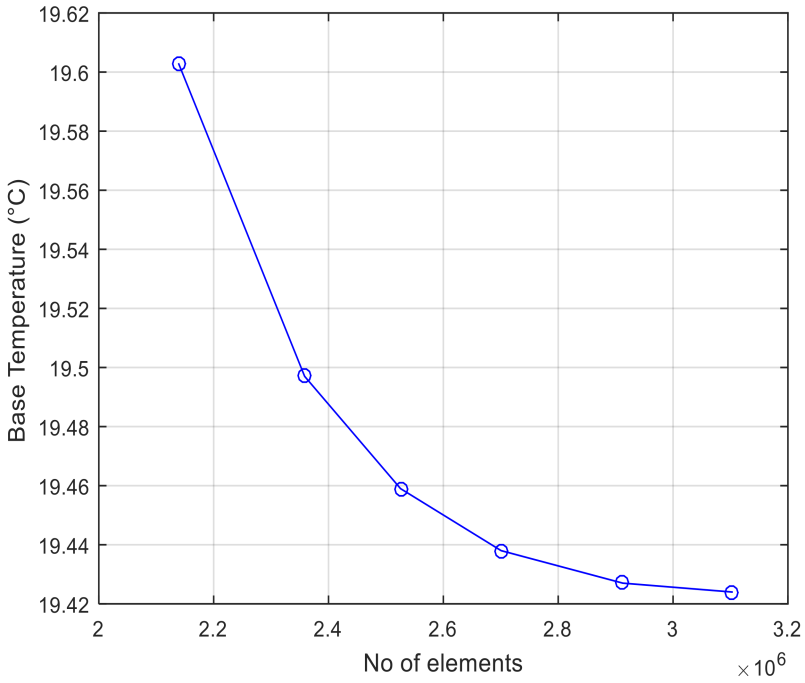

Figure 2. Temperature difference with number of elements.

2.4. Heat Sink

The heat sink was designed on an ANSYS Design Modeler. All of the heat sinks were modeled according to dimensions obtained in the literature [1]. A cubic chip was made at the bottom of the heat sink with dimensions of 28.7 mm × 28.7 mm × 0.5 mm in order to provide 325 W of heat. The dimensions of two SPFMCHSs with 1 mm fin spacing are shown in Figure 3. The details of all the cases solved in this numerical study are provided in Table 1. The isometric view of two SPFMCHSs, three SPFMCHSs, and SIFMCHSs, along with a co-ordinate axis, is shown in Figure 4. SIFMCHSs with varying fin spacings of 0.5 mm, 1 mm, and 1.5 mm are shown in Figure 5. The propagation of flow through two SPFMCHSs from the inlet to outlet is shown in Figure 6.

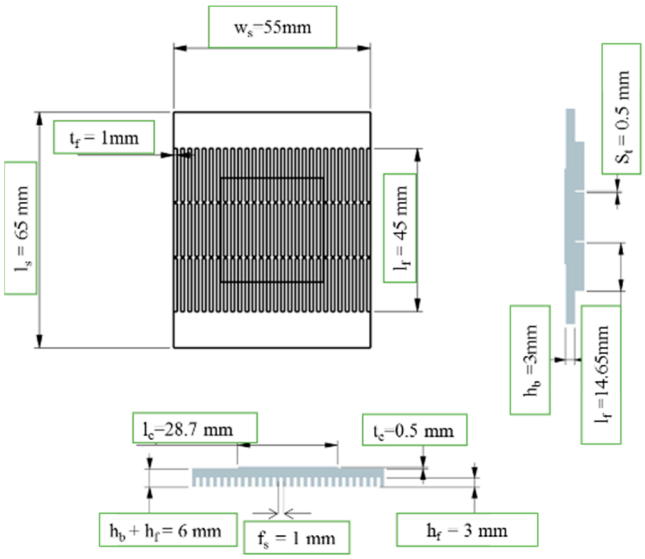

Figure 3. Dimensions of two SPFMCHSs with 1 mm fin spacing.

Table 1. Detail of cases solved with numerical simulations.

No. of Slots Per Fin	f_s (mm)	t_f (mm)	h_f (mm)	S_t (mm)
2	0.5	1	3	0.5
2	1	1	3	0.5
2	1.5	1	3	0.5
3	0.5	1	3	0.5
3	1	1	3	0.5
3	1.5	1	3	0.5

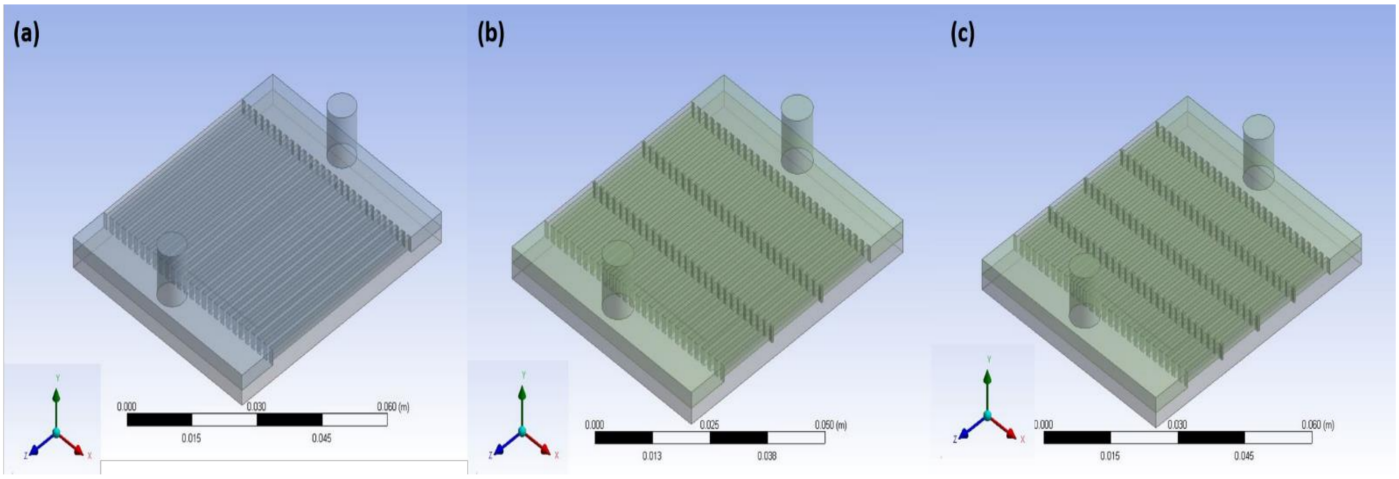

Figure 4. Isometric views for 0.5 mm fin spacing: (**a**) SIFMCHS [1], (**b**) two SPFMCHSs, and (**c**) three SPFMCHSs.

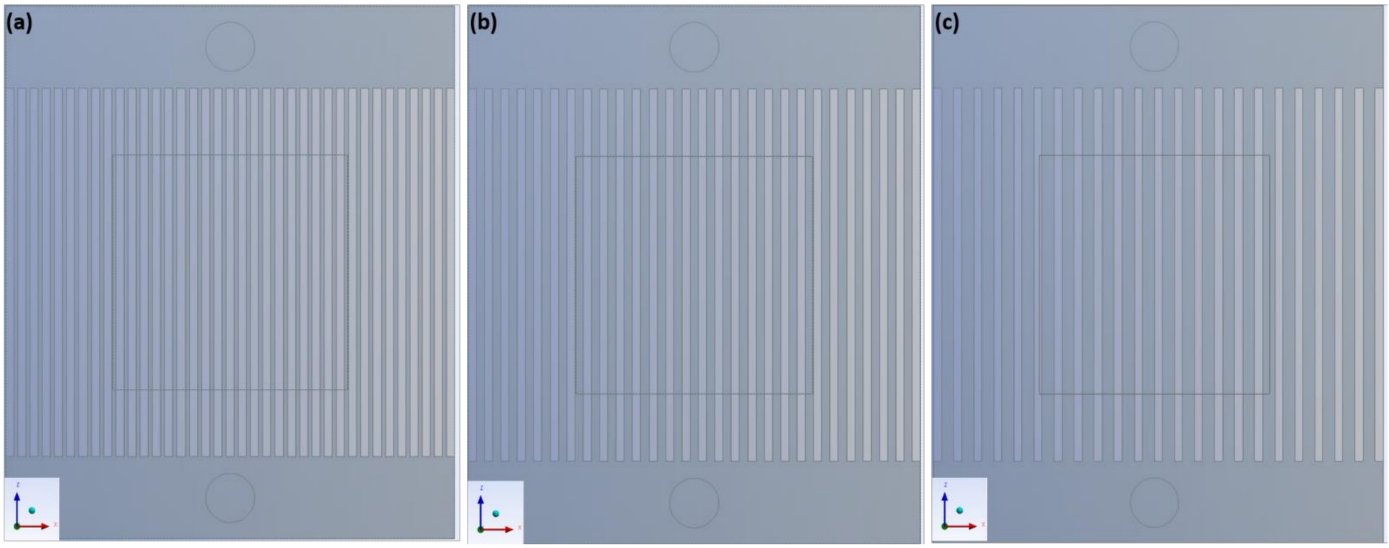

Figure 5. SIFMCHSs: (**a**) 0.5 mm, (**b**) 1 mm, and (**c**) 1.5 mm fin spacing.

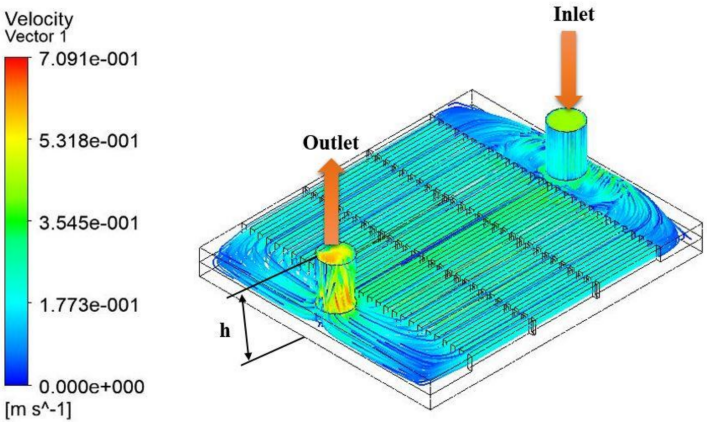

Figure 6. Propagation of flow through two SPFMCHSs.

2.5. Uniformity in Temperature Distribution

For the longer operation and durability of electronic devices, temperature uniformity was essential. All cases that were examined had a uniform temperature distribution inside the heat sink. The contours of the base temperature for two SPFMCHSs and three SPFMCHSs are shown in Figures 7 and 8.

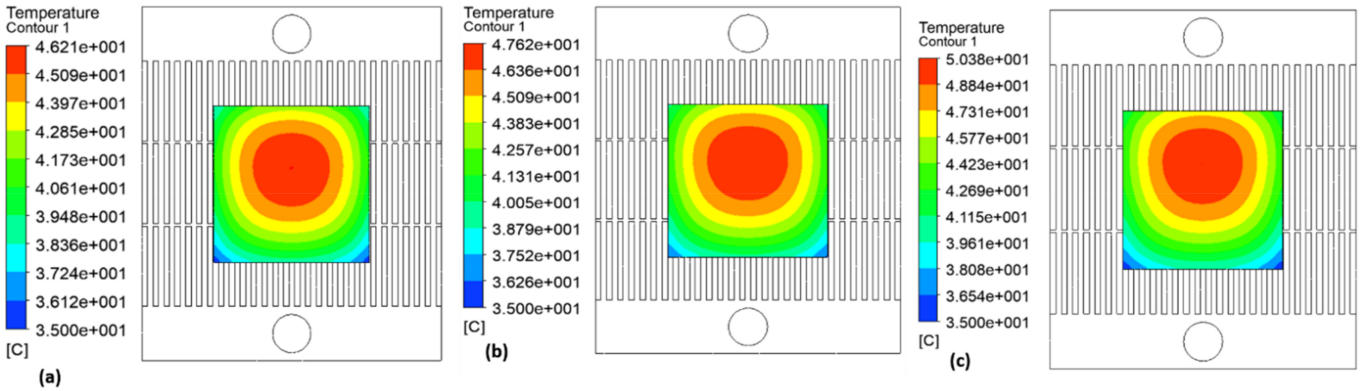

Figure 7. Base temperature distribution of two SPFMCHSs with 1 mm fin spacing: (**a**) 0.5 LPM, (**b**) 0.75 LPM, and (**c**) 1 LPM.

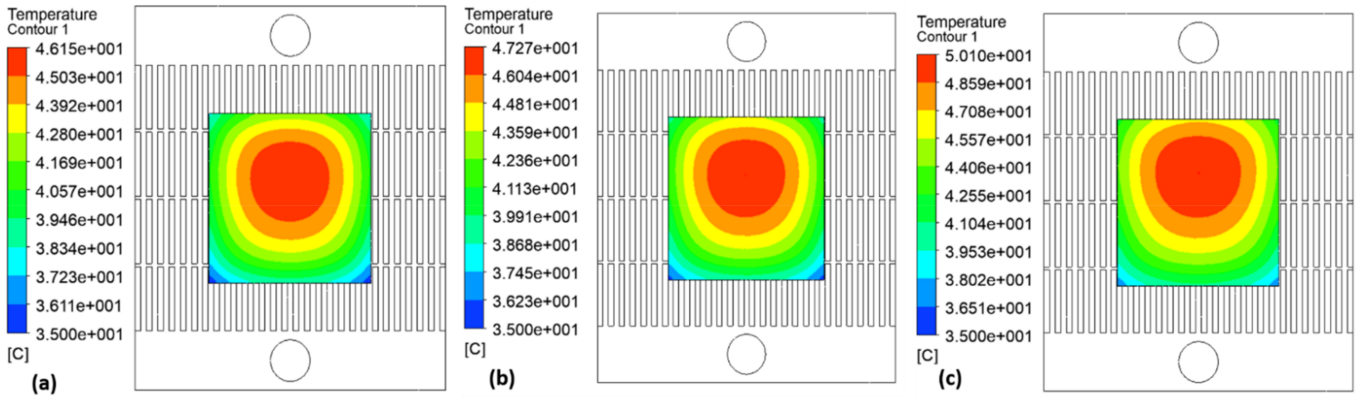

Figure 8. Base temperature distribution of three SPFMCHSs with 1 mm fin spacing: (**a**) 0.5 LPM, (**b**) 0.75 LPM, and (**c**) 1 LPM.

2.6. Selection of Slot Thickness

The flow becomes developed at one quarter of the distance from the entrance between the fins of heat sink. At this stage, the fluid velocity reaches the maximum at the center and the minimum at the boundaries of the flow. To reinitialize the velocity boundary layer, slots were added into the straight integral fins. This made a good contact between the flow and fins. The fully developed flow in between the fins in a 2D plane is shown in Figure 9. The slots were of varying thickness from 0.3 mm up to 1 mm, and the base temperature was recorded against each slot thickness. The thickness of the slot was selected finally as 0.5 mm for both the cases (two and three SPFMCHSs), as the minimum base temperature was recorded using 0.5 mm-thick slots. The formation of vortices took place inside the slots. This led to turbulence and enhanced heat transfer. There was a notable increment in the base temperature recorded for slot thicknesses of 0.5 mm to 0.6 mm. This is the point where the base temperature started to increase instead of decrease. The details are shown in Figure 10. The temperature distribution for two and three SPFMCHSs with 1 mm fin spacing is shown in Figures 7 and 8.

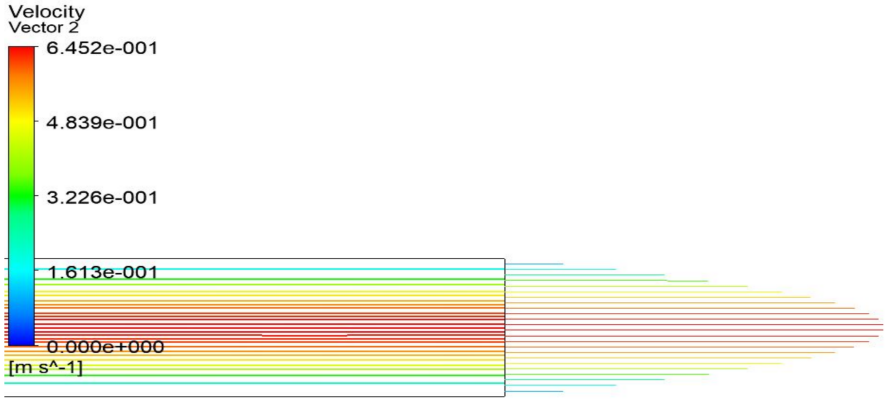

Figure 9. Two-dimensional pictorial view of the fully developed flow in between the fins.

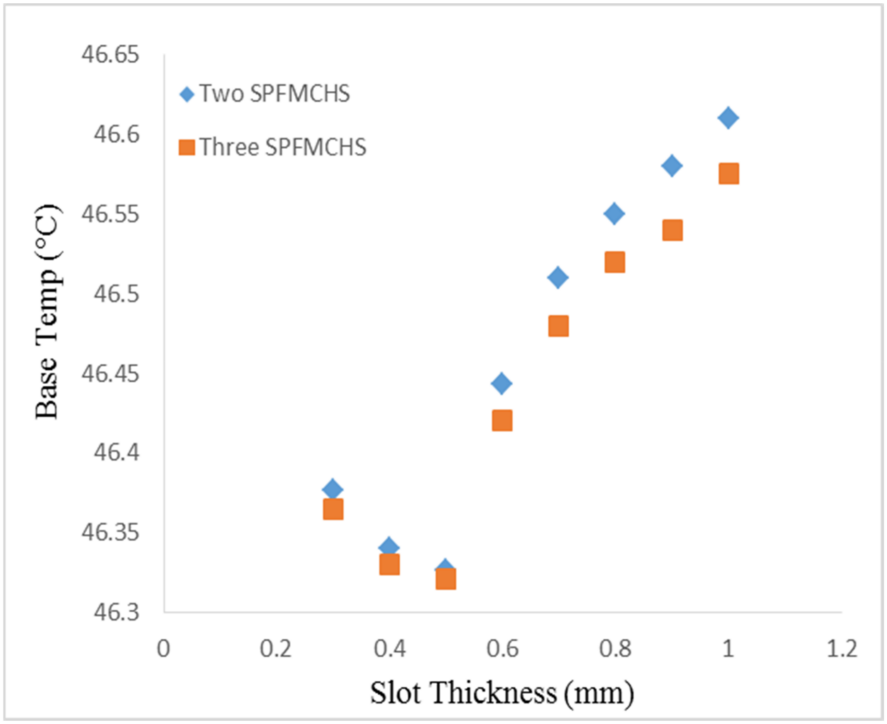

Figure 10. Base temp vs. slot thickness.

3. Results and Discussion

3.1. Heat Transfer

A direct relation was observed between the flow rate and the heat transfer, as shown in Figure 11. The graph shows that heat transfer is dependent on fin spacing and the number of slots. Increasing fin spacing resulted in a reduction in heat transfer. The maximum heat transfer observed in two SPFMCHSs, with 0.5 mm fin spacing, was 316 W at 1 LPM. The minimum heat transfer rate observed in three SPFMCHSs, with 1.5 mm fin spacing, was 280 W at 0.5 LPM. The heat sinks with two SPFMCHSs showed a higher heat transfer as compared to three SPFMCHSs with varying LPM and fin spacings. There was little difference in the heat transfer recorded for two and three SPFMCHSs with 1 mm fin spacing. When comparing two SPFMCHSs to three SPFMCHSs at 1 LPM, the percentage enhancement in heat transfer recorded for 0.5 mm, 1 mm, and 1.5 mm fin spacings was 0.95%, 0.32%, and 0.68%, respectively.

3.2. Base Temperature Drop

The base temperature drop for two and three SPFMCHSs was calculated by subtracting the base temperature of a conventional SIFMCHS [1] from two and three SPFMCHSs with varying fin spacings and LPM, as shown in Figure 12. The maximum temperature drop was recorded in two and three SPFMCHSs with 1 mm fin spacing. The maximum base temperature drop value was 6.31 °C for three SPFMCHSs with 1 mm fin spacing at 0.5 LPM. The minimum base temperature drop value was 3.14 °C for three SPFMCHSs with 1.5 mm fin spacing.

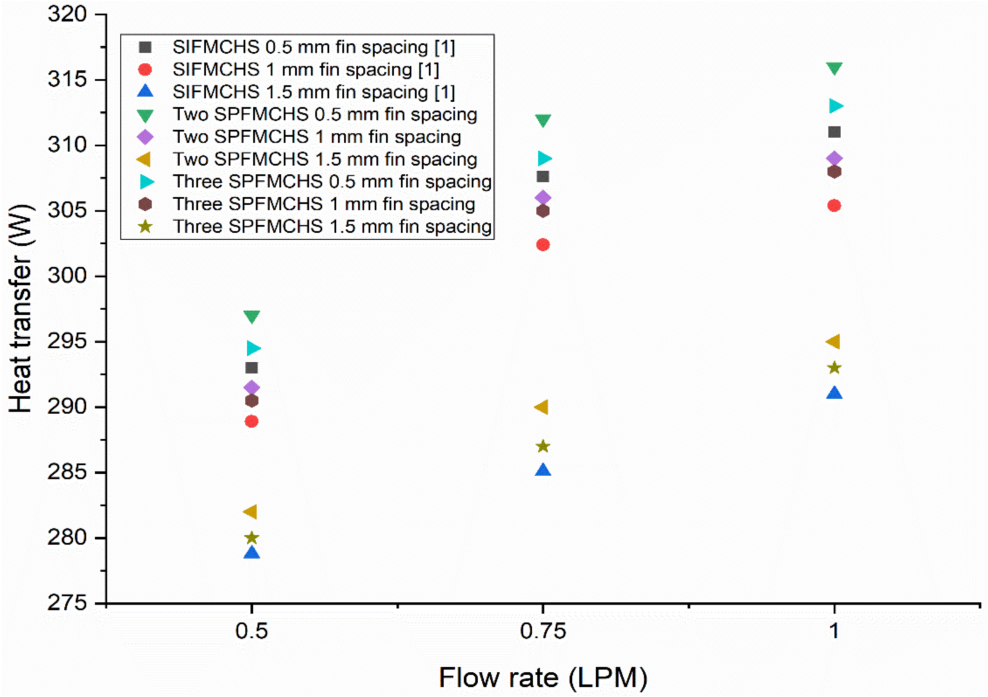

Figure 11. Heat transfer with volumetric flow rate.

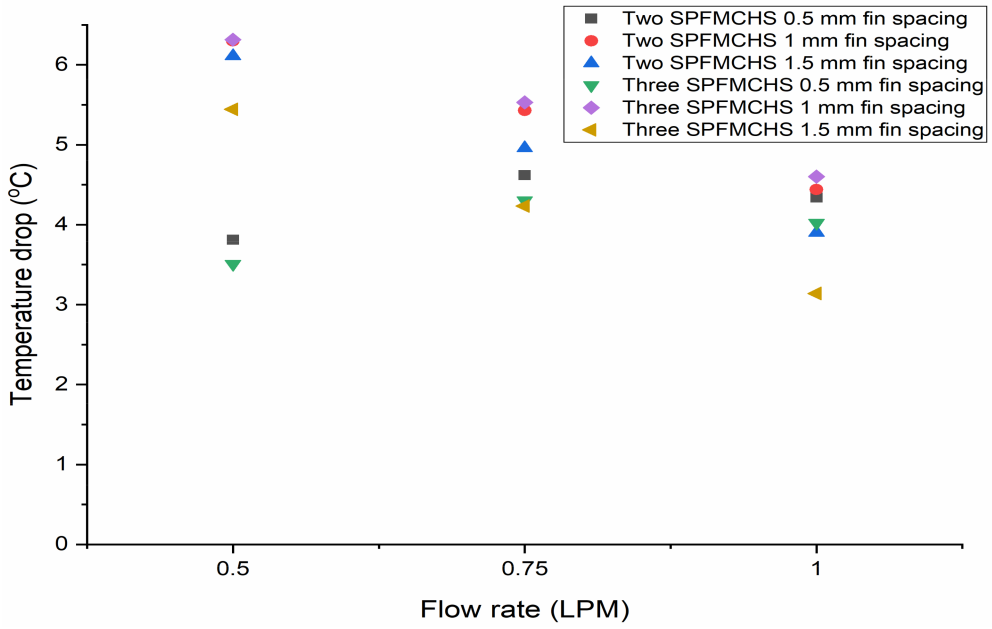

Figure 12. Temperature drop with volumetric flow rate.

3.3. Base Temperature

The base temperatures of SPFMCHSs at different volumetric flow rates are shown in Figure 13. The base temperature increases by increasing the fin spacing as the active area of the heat sink decreases. The minimum base temperature noted for two SPFMCHSs with 0.5 mm fin spacing was 42.81 °C at 1 LPM. The maximum base temperature, observed in two SPFMCHSs with 1.5mm fin spacing, was 53.51 °C at 0.5 LPM. An inverse relation was observed between the flow rate and the base temperature. The reduction in base temperature using SPFMCHSs was greater than that in SIFMCHSs [1]. This clearly highlights the importance of making slots in straight integral fins. The base temperature recorded for two SPFMCHSs with 0.5 mm and 1.5 m fin spacings was lower than for three SPFMCHSs

with the same fin spacing. For three SPFMCHSs, the percentage reduction in the base temperature was recorded as 8.53%, 9%, and 5.95% for 0.5 mm, 1 mm, and 1.5 mm fin spacings, respectively, compared to SIFMCHSs [1] at 1 LPM with the same fin spacing. The base temperature recorded in two SPFMCHSs with 0.5 mm, 1 mm, and 1.5 mm fin spacings at 1 LPM was 42.81 °C, 46.36 °C, and 48.87 °C, respectively, which is 9.20%, 8.74%, and 7.39% lower than the reported values in the literature [1] for SIFMCHSs. The base temperature distribution is shown in Figures 7 and 8 for two and three SPFMCHSs, respectively, with 1 mm fin spacing.

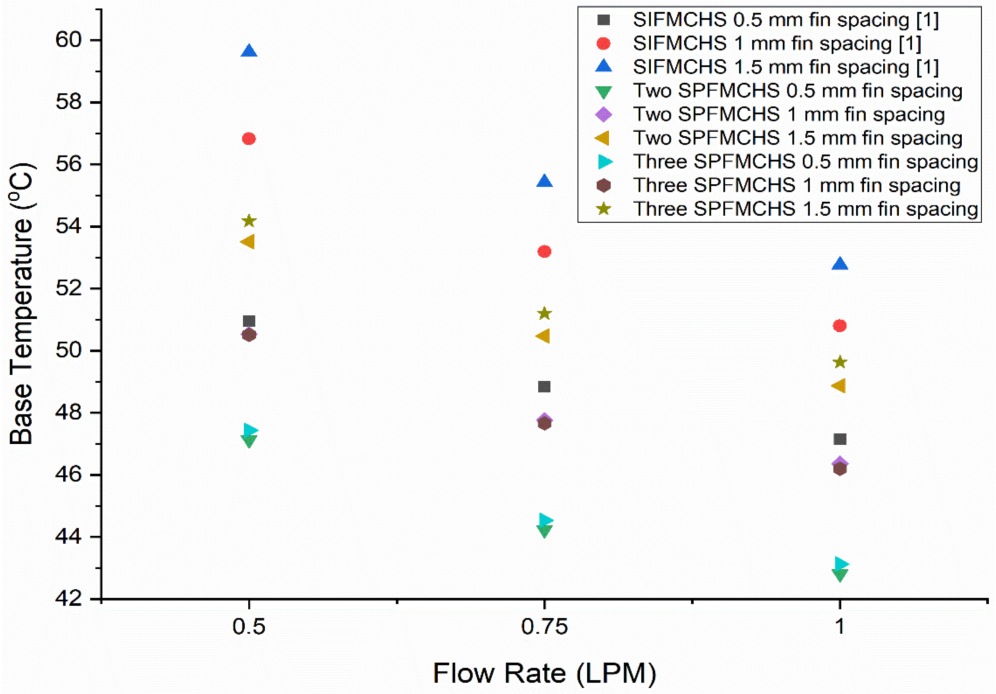

Figure 13. Base temperature with volumetric flow rate.

3.4. Pressure Drop

The pressure drops observed for SPFMCHSs across various volumetric flow rates are shown in Figure 14. By increasing the flow rate, the pressure drop increases. An inverse relationship was observed between the flow rate and the pressure drop. Increasing fin spacing results in a decreased pressure drop at varying LPM. The pressure drops recorded for two and three SPFMCHSs with varying fin spacings were found to be equal. The percentage reduction in the pressure drop observed at 0.5 mm, 1 mm, and 1.5 mm fin spacings for two SPFMCHSs was 0.64%, 20.68%, and 27.12% respectively, when compared to SIFMCHSs at 1 LPM. The percentage difference noted for three SPFMCHSs was 1.50%, 21.26%, and 27.93% at 0.5 mm, 1 mm, and 1.5 mm fin spacings, respectively, when compared to SIFMCHs. The minimum pressure drops recorded for two SPFMCHSs and three SPFMCHSs with 1.5 mm fin spacing were 356.7 Pa and 352.68 Pa, respectively, at 0.5 LPM. The maximum pressure drops recorded for two and three SPFMCHSs with 0.5 mm fin spacing were 1127.65 Pa and 1117.96 Pa, respectively, at 1 LPM. The pumping power increases as the pressure drops to maintain the desired flow rate. The pressure drops recorded for two and three SPFMCHSs with 0.5 mm fin spacing at varying LPM were found to be equal to the reported value in [1] for SIFMCHSs.

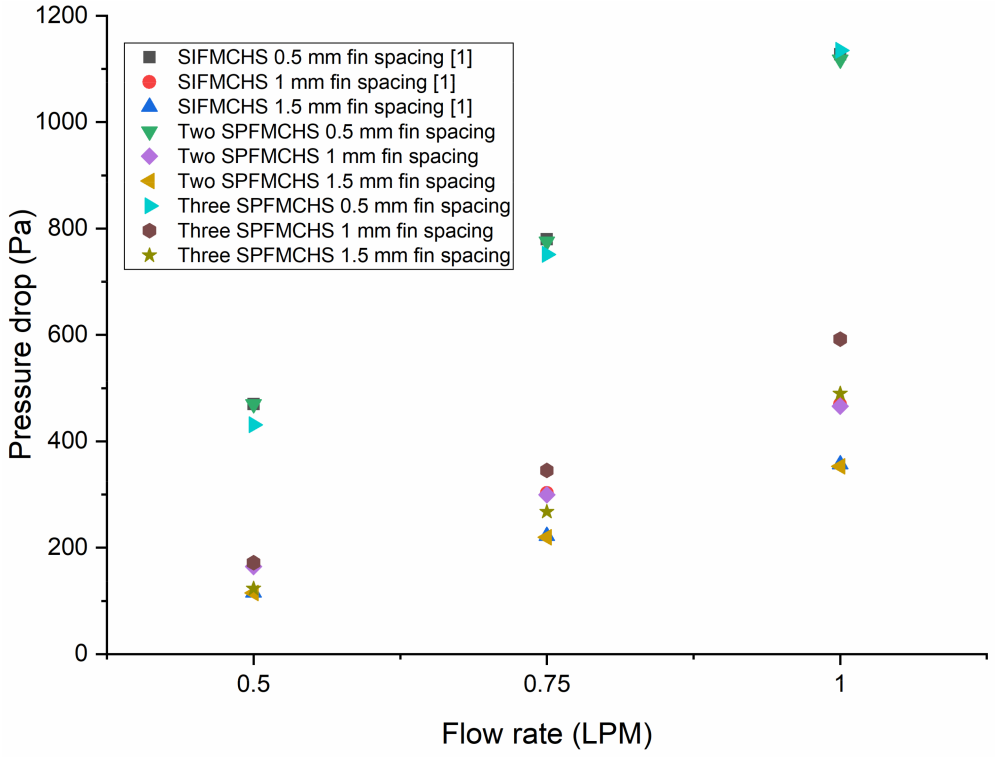

Figure 14. Pressure drop with volumetric flow rate.

3.5. Thermal Resistance

The effect of thermal resistance with volumetric flow rate for SPFMCHSs with two and three SPFMCHSs is shown in Figure 15. The thermal resistance decreases as the flow rate increases. By increasing the fin spacing, the thermal resistance also increases. The minimum thermal resistance recorded in two SPFMCHSs with 0.5 mm fin spacing was 0.036 °C/W at 1 LPM. A similar level of thermal resistance was recorded in two and three SPFMCHSs with various fin spacings. The maximum thermal resistance was recorded in three SPFMCHSs with 1.5 mm fin spacing at 0.5 LPM. The reduction in thermal resistance was recorded as 11.24%, 4.48%, and 8.80% in two SPFMCHSs with 0.5 mm, 1 mm, and 1.5 mm fin spacings, respectively, as compared to the reported values for SIFMCHSs [1] at 1 LPM. The reduction in thermal resistance was observed as 6.31%, 4.83%, and 7.83% in three SPFMCHSs with 0.5 mm, 1 mm, and 1.5 mm fin spacings, respectively, as compared to the reported values for SIFMCHSs [1] at 1 LPM.

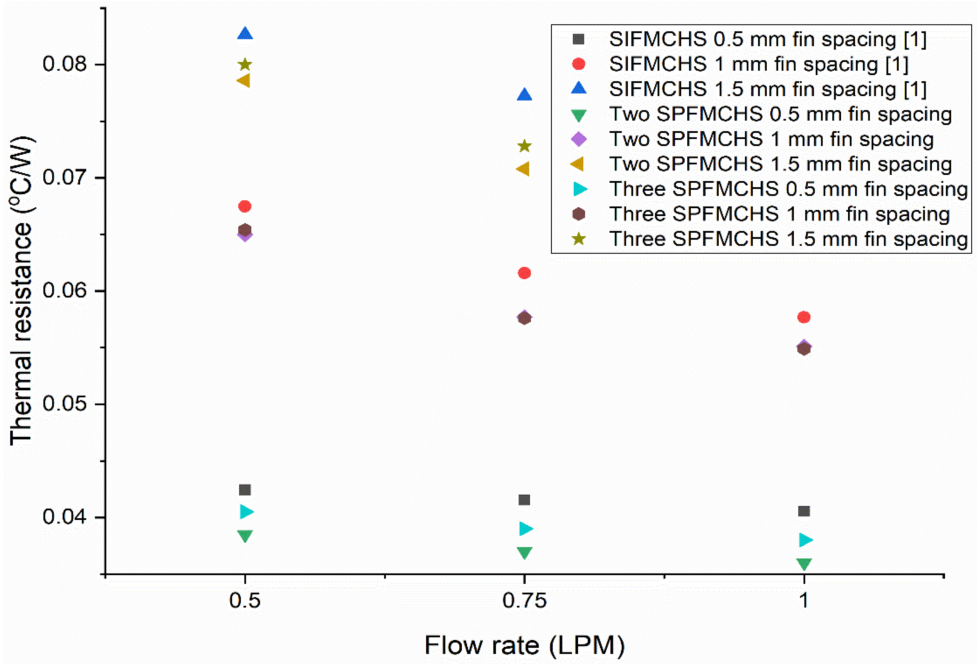

Figure 15. Thermal resistance with volumetric flow rate.

4. Conclusions

A thermal investigation of SPFMCHSs with fin spacings of 0.5 mm, 1 mm, and 1.5 mm was conducted numerically and compared to the SIFMCHS, using water as the cooling fluid, present in the literature. The findings of this detailed numerical study are:

- The base temperature recorded in two SPFMCHSs with 0.5 mm, 1 mm, and 1.5 mm fin spacings at 1 LPM was 42.81 °C, 46.36 °C, and 48.869 °C, respectively. This was 9.20%, 8.74%, and 7.39%, respectively, less than the SIFMCHSs. The minimum base temperature was recorded in two SPFMCHSs with 0.5 mm fin spacing, and the maximum base temperature was recorded in SIFMCHSs with a fin spacing of 1.5 mm at varying LPM. The reduction in the base temperature recorded for 0.5 mm, 1 mm, and 1.5 mm in two SPFMCHSs was 9.2%, 7.61%, and 7.39%, respectively, and in three SPFMCHSs was 8.23%, 7.22%, and 5.95%, respectively, from the reported value in the literature [1].
- The maximum heat transfer was recorded in two SPFMCHSs as compared to three SPFMCHSs with 0.5 mm fin spacing. The minimum heat transfer recorded was for 1.5 mm fin spacing in three SPMCHSs at 0.5 LPM. The percentage increase in the heat transfer recorded for 0.5 mm,1 mm, and 1.5 mm in two SPFMCHSs was 1.6%, 1.16%, and 1.02%, respectively, and for three SPFMCHSs was 0.64%, 0.52%, and 0.44 %, respectively, from the reported value in the literature [1].
- The percentage reduction in the base temperature recorded in three SPFMCHSs with 0.5 mm, 1 mm, and 1.5 mm fin spacings at 1 LPM was 8.53%, 9%, and 5.95%, respectively, when compared to SIFMCHSs.
- The reduction in the thermal resistance was observed as 11.24%, 4.48%, and 8.80% in two SPFMCHSs with 0.5 mm, 1 mm, and 1.5 mm fin spacings, respectively, when compared to SIFMCHSs at 1 LPM. The minimum thermal resistance was recorded in two SPFMCHSs with 0.5 mm fin spacing, and the maximum thermal resistance was recorded in SIFMCHSs with 1.5 mm fin spacing.
- The reduction in the thermal resistance was observed to be 6.31%, 4.83%, and 7.83% in three SPFMCHSs with 0.5 mm, 1 mm, and 1.5 mm fin spacings when compared to SIFMCHSs at 1 LPM. The reduction in the thermal resistance recorded for 0.5 mm, 1 mm, and 1.5 mm fin spacings in two SPFMCHSs was 11.33%, 9.1%, and 8.83%, respectively, from the reported value in the literature [1]. In three SPFMCHSs, the

reduction in the thermal resistance for fin spacings of 0.5 mm, 1 mm, and 1.5 mm was 6.40%, 5.84%, and 4.85%, respectively, from the reported value in the literature.

- The percentage reduction in the pressure drop observed for 0.5 mm, 1 mm, and 1.5 mm fin spacings in two SPFMCHSs was 0.64%, 20.68%, and 27.12%, respectively, as compared to SIFMCHSs at 1 LPM. The percentage difference noted in three SPFMCHSs was 1.50%, 21.26%, and 27.93% at 0.5 mm, 1 mm, and 1.5 mm fin spacings, respectively, when compared to SIFMCHS.

Author Contributions: Conceptualization, Z.R. and H.A.T.; Data curation, T.B., M.A. and H.P.; Formal analysis, M.A.; Funding acquisition, K.R. and H.P.; Investigation, Z.R., H.A.T. and A.W.; Methodology, T.B. and Z.R.; Project administration, H.A.T., S.M. and A.W.; Resources, S.M. and K.R.; Supervision, Z.R.; Validation, Z.R.; Writing—original draft, T.B.; Writing—review and editing, Z.R. and H.P. All authors have read and agreed to the published version of the manuscript.

Funding: This research was funded by the Basic Science Research program through the National Research Foundation of Korea (NRF) funded by the ministry of Education, grant number 2020R1I1A1A01073797.

Conflicts of Interest: The authors declare no conflict of interest.

Nomenclature

C_p	= specific heat, kJ/kg °C
w_s	= width of heat sink, mm
l_s	= length of heat sink, mm
l_f	= length of fin, mm
t_f	= Thickness of fin, mm
S_t	= slot thickness, mm
h_b	= height of heat sink base plate, mm
h_f	= height of fin, mm
l_c	= length of chip, mm
t_c	= thickness of chip, mm
l_t	= total length, mm
f_s	= fin spacing, mm
LMTD	= log of mean temperature difference, °C
$\dot{m}$	= mass flow rate, kg/s
$\dot{Q}$	= heat transfer rate, W
R_{th}	= thermal resistance, °C/W
T_b	= base temperature, °C
T_i	= fluid inlet temperature, °C
T_o	= fluid outlet temperature, °C

Abbreviations

SFMCHS	= slotted fin minichannel heat sink
SIFMCHS	= straight integral fin minichannel heat sink
SPFMCHS	= slots per fin minichannel heat sink
LPM	= liters per minute

References

1. Saeed, M.; Kim, M.H. Numerical study on thermal hydraulic performance of water cooled mini-channel heat sinks. *Int. J. Refrig.* **2016**, *69*, 147–164. [CrossRef]
2. Tuckerman, D.B.; Pease, R.F. High-Performance Heat Sinking for VLSI. *IEEE Electron. Device Lett.* **1981**, *EDL-2*, 126–129. [CrossRef]
3. Huang, S.; Zaho, J.; Gong, L.; Duan, X. Thermal performance and structure optimization for slotted microchannel heat sink. *Appl. Therm. Eng.* **2016**, *115*, 1266–1276. [CrossRef]
4. Knight, R.W.; Hall, D.J.; Goodling, J.S.; Jaeger, R.C. Heat Sink Optimization with Application. *IEEE Trans. Compon. Hybrids Manuf. Technol.* **1992**, *5*, 832–842. [CrossRef]
5. Gawali, B.S.; Swami, V.B.; Thakre, S.D. Theoretical and Experimental Investigation of Heat Transfer Characteristics through a Rectangular Microchannel Heat Sink. *Int. J. Innov. Res. Sci. Eng. Technol.* **2014**, *3*, 8. [CrossRef]
6. Wang, X.D.; An, B.; Xu, J.L. Optimal geometric structure for nanofluid-cooled microchannel heat sink under various constraint conditions. *Energy Convers. Manag.* **2013**, *65*, 528–538. [CrossRef]

7. Hung, T.C.; Huang, Y.X.; Yan, W.M. Thermal performance analysis of porous-microchannel heat sinks with different configuration designs. *Int. J. Heat Mass Transf.* **2013**, *66*, 235–243. [CrossRef]
8. Gunnasegaran, P.; Mohammed, H.A.; Shuaib, N.H.; Saidur, R. The effect of geometrical parameters on heat transfer characteristics of microchannels heat sink with different shapes. *Int. Commun. Heat Mass Transf.* **2010**, *37*, 1078–1086. [CrossRef]
9. Qu, W.; Mala, G.m.; Li, D. Heat tranfer for water flow in trapezoidal silicon microchannel. *Int. J. Heat Mass Transf.* **2000**, *43*, 3925–3936. [CrossRef]
10. Kumar, N.; Singh, N.K. Study and Analysis on Micro Channel Heat Sink in Trapezoidal Shape. *Int. J. Curr. Eng. Technol.* **2017**, *7*, 1115–1118.
11. Xie, X.L.; Tao, W.Q.; He, Y.L. Numerical study of turbulent heat transfer and pressure drop characteristics in water cooled mini channel heat sink. *J. Electron. Packag.* **2007**, *129*, 247–255. [CrossRef]
12. Dixit, T.; Ghosh, I. Low Reynolds number thermo-hydraulic characterization of offset. *Exp. Therm. Fluid Sci.* **2013**, *51*, 227–238. [CrossRef]
13. Saini, M.; Webb, R.L. Heat Rejection Limits of Air Cooled Plane Fin Heat. *IEEE Trans. Compon. Packag. Technol.* **2003**, *26*, 71–79. [CrossRef]
14. Naphon, P.; Wiriyasart, S. Liquid cooling in the mini-rectangular fin heat sink with and without thermoelectric for CPU. *Int. Commun. Heat Mass Transf.* **2009**, *36*, 166–171. [CrossRef]
15. Saeed, M.; Kim, M.H. Heat Tranfer enhancement using Nano fluids (Al_2O_3-H_2O) in mini channel heat sink. *Int. J. Heat Mass Tranafer* **2018**, *120*, 671–682. [CrossRef]
16. Al-Tae'y, K.A.; Ali, E.H.; Jebur, M.N. Experimental Investigation of Water Cooled Minichannel Heat Sink for Computer Processing Unit Cooling. *Int. J. Eng. Res. Appl.* **2017**, *7*, 38–49.
17. Yu, X.; Feng, J.; Feng, Q.; Wang, Q. Development of a plate-pin fin heat sink and its performance comparisons with a plate fin heat sink. *Appl. Therm. Eng.* **2005**, *25*, 173–182. [CrossRef]
18. Tariq, H.A.; Israr, A.; Khan, Y.I.; Anwar, M. Numerical and experimental study of cellular structures as a heat dissipation media. *Heat Mass Transf.* **2019**, *55*, 510–511. [CrossRef]
19. Tariq, H.A.; Shoukat, A.A.; Anwar, M.; Ali, H.M. Water Cooled Micro-hole Cellular Structure as a Heat Dissipation Media: An Experimental and Numerical Study. *Therm. Sci.* **2018**, *2018*, 184. [CrossRef]
20. Tariq, H.A.; Shoukat, A.A.; Hassan, M.; Anwar, M. Thermal management of microelectronic devices using micro-hole cellular structure and nanofluids. *J. Therm. Anal. Calorim.* **2019**, *136*, 2171–2182. [CrossRef]
21. Valueva, E.P.; Purdin, M.S. The pulsating laminar flow in a rectangular channel. *Thermophys. Aeromechanics* **2015**, *22*, 733–744. [CrossRef]
22. Valueva, E.P.; Purdin, M.S. Heat exchange at laminar flow in rectangular channels. *Thermophys. Aeromechanics* **2016**, *23*, 857–867. [CrossRef]
23. Khoshvaght-Aliabadi, M.; Hassani, S.M.; Mazloumi, S.H. Comparison of hydrothermal performance between plate fins and plate-pin fins subject to nanofluid-cooled corrugated miniature heat sinks. *Microelectron. Reliab.* **2017**, *70*, 84–96. [CrossRef]
24. Rezaee, M.; Khoshvaght-Aliabadi, M.; Arani, A.A.A.; Mazloumi, S.H. Heat transfer intensification in pin-fin heat sink by changing pin-length/longitudinal-pitch. *Chem. Eng. Process.-Process. Intensif.* **2019**, *141*, 107544. [CrossRef]
25. Khoshvaght-Aliabadi, M.; Hassani, S.M.; Mazloumi, S.H. Performance enhancement of straight and wavy miniature heat sinks using pin-fin interruptions and nanofluids. *Chem. Eng. Process.* **2017**, *122*, 90–108. [CrossRef]
26. Ali, M.; Shoukat, A.A.; Tariq, H.A.; Anwar, M.; Ali, H. Header Design Optimization of Mini-channel Heat Sinks Using CuO–H_2O andAl_2O_3–H_2O Nanofluids for Thermal Management. *Arab. J. Sci. Eng.* **2019**. [CrossRef]
27. Wang, W.; Li, Y.; Zhang, Y.; Li, B.; Sundén, B. Analysis of laminar flow and heat transfer in an interrupted microchannel heat sink with different shaped ribs. *J. Therm. Anal. Calorim.* **2020**, *140*, 1259–1266. [CrossRef]
28. Tran, N.G.R.; Chang, Y.; Teng, J. A study on five different channel shapes using a novel scheme for meshing and a structure of a multi-nozzle microchannel heat sink. *Int. J. Heat Mass Transf.* **2017**, *105*, 429–442. [CrossRef]